Hindawi
Advances in Materials Science and Engineering
Volume 2017, Article ID 3571454, 6 pages
https://doi.org/10.1155/2017/3571454

Research Article

Influence of Elements on the Corrosion Resistance of DLC Films

Nutthanun Moolsradoo[1] and Shuichi Watanabe[2]

[1]*King Mongkut's University of Technology Thonburi, Bangkok 10140, Thailand*
[2]*Nippon Institute of Technology, Saitama 345-8501, Japan*

Correspondence should be addressed to Nutthanun Moolsradoo; nutthanun.moo@kmutt.ac.th

Received 12 February 2017; Revised 1 May 2017; Accepted 24 May 2017; Published 20 June 2017

Academic Editor: Angela De Bonis

Pure DLC, Si-DLC, and Si-N-DLC films deposited from C_2H_2, C_2H_2 : TMS and C_2H_2 : TMS : N_2 mixtures were used to study the effects of the elemental contents (silicon, silicon-nitrogen) on deposition and corrosion resistance properties. The films were prepared on Si (100) wafers using the plasma-based ion implantation (PBII) technique. The film structure was analyzed using Raman spectroscopy. The composition at the top surface of the films was measured using energy dispersive X-ray spectroscopy (EDS). The hardness and elastic modulus of the films were measured using a nanoindentation hardness tester. The corrosion performance of the films was conducted using potentiodynamic polarization experiments in an aqueous 0.05 M NaCl solution. The results indicate that the hardness and corrosion resistance of the Si-DLC film increase as the silicon content increases. This is due to the increase of the sp^3 cluster. The corrosion resistance of a pure DLC film increases when silicon and silicon-nitrogen are doped into the film. Si-DLC films with a silicon content of 40 at.% had a corrosion potential value of 0.61 V, while a Si-N-DLC film with a silicon and nitrogen content of 19.3 at.% and 1 at.% shows a corrosion potential value of 0.85 V, which is a considerable improvement in the corrosion resistance property.

1. Introduction

Diamond-like carbon (DLC) films are a metastable form of amorphous carbon that have a unique combination of properties, such as high hardness and elastic modulus, good wear resistance, and a low friction coefficient. Because of its special properties, it is commonly applied as a wear-resistant protective coating in the magnetic storage, automobile, tooling, biomedical, and other industries [1–3]. Another good property reported is the DLC electrochemical resistance [4–6]. DLC electrochemical corrosion behavior is known to be dependent on the film composition and structure, which depend on the deposition technique and precursor gas [4]. Many investigations have been dedicated to the introduction of additional foreign elements in the structure to improve the properties of DLC coatings [7, 8].

The plasma-based ion implantation (PBII) technique was developed to improve the properties of DLC films [9]. The samples are immersed in plasma and biased to a negative potential. A plasma sheath then forms and accelerated ions bombard the exposed surface of the samples.

DLC coatings have been reported to improve the corrosion protection properties, and a silicon-doped DLC with a silicon content of up to 20.2 at.% prepared using the PECVD process can significantly improve the corrosion properties. This is due to the formation of a passivation layer, which fills the pores present in the films [10, 11]. In [12–14] by Choi et al., silicon-doped DLC coatings improved the corrosion protection properties, especially in the case silicon-doped DLC films prepared using an electron cyclotron resonance (ECR) technique. Zeng et al. [15] reported that the corrosion resistance of DLC films decreased with an increase in the working temperature, showing that the sp^2/sp^3 ratio has an apparent effect on the corrosion resistance of the DLC film. Hatada et al. [16] reported that oxygen and nitrogen implantations improved the corrosion protection properties of DLC fabricated from N_2, O_2, and C_2H_4 gases. In [17] by Masami et al., Si-DLC prepared on an alloy exhibited a high corrosion resistance.

Currently, there have been no reports of the deposition of DLC film doped with different silicon and silicon-nitrogen ratios using the PBII technique, aimed at comparing the

Table 1: Deposition of pure DLC, Si-DLC, and Si-N-DLC films.

Film type	Gaseous mixture	Bias voltage (kV)	RF power (W)	Deposition pressure (Pa)	Gas flow rate ratio	Actual gas flow (sccm)
Pure DLC	C_2H_2	−5	300	2	—	18
Si-DLC	C_2H_2 : TMS	−5	300	2	2 : 1	11.4 : 5.7
					1 : 4	3.7 : 14.8
Si-N-DLC	C_2H_2 : TMS : N_2	−5	300	2-3	14 : 1 : 1	14 : 1 : 1
					14 : 1 : 2	14 : 1 : 2
					14 : 1 : 3	14 : 1 : 3

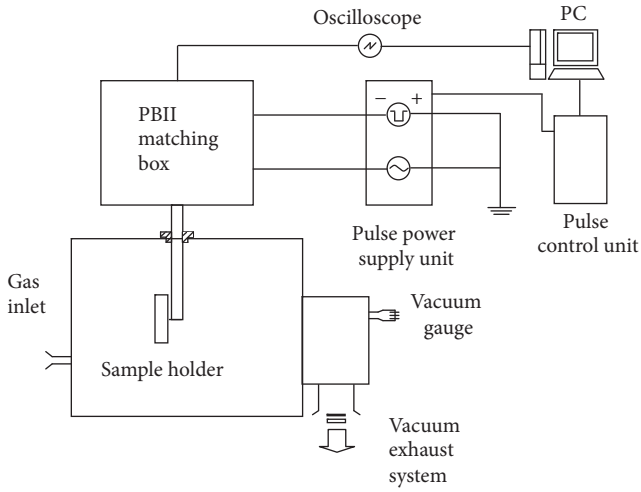

Figure 1: Schematic of the PBII apparatus used in this experiment [18–20].

mechanical properties and corrosion resistances. In this paper, plasma-based ion implantation (PBII) was utilized to prepare different elements including silicon and silicon-nitrogen (henceforth referred to as Si-DLC and Si-N-DLC films). The aim of this study was to study the effects of the elemental contents on the deposition, mechanical properties, and corrosion resistance of the films.

2. Experimental Details

A schematic of the plasma-based ion implantation (PBII) apparatus is shown in Figure 1 [18–20]. The inner dimensions of the vacuum chamber were $600 \times 630 \times 200\ mm^3$, with a residual pressure of approximately 1×10^{-4} Pa. The plasma was generated by a radio frequency (RF, 13.6 MHz) glow discharge and a negative high voltage pulse power supply that was connected to the sample holder.

Silicon (100) wafers with a thickness of 0.7 mm were used as substrates. All silicon substrates were prepared by sputter-cleaning and then interlayer deposition using PBII apparatus. The substrate was sputter-cleaned with Ar^+ for 20 min to remove surface contaminants. Then, the interlayer was first deposited with CH_4 for 60 min to improve the adhesion between the film and the substrate. The negative pulse bias voltage of the sputter-cleaning and interlayer deposition was set to −10 kV and −20 kV, respectively. The RF power and pressure of the sputter-cleaning and the interlayer deposition were set to 300 W and 1 Pa, respectively. The pulse frequency of the sputter-cleaning and the interlayer deposition was set to 1 kHz at a pulse width of 5 μs and a pulse delay of 25 μs and 60 μs.

The pure DLC, Si-DLC, and Si-N-DLC films were prepared using the PBII technique. The pure DLC film was deposited using a C_2H_2 precursor gas. The Si-DLC film was deposited from gaseous mixtures of C_2H_2 : TMS, at two different flow rate ratios of 2 : 1 and 1 : 4. The Si-N-DLC film was deposited from gaseous mixtures of C_2H_2 : TMS : N_2 at three different flow rate ratios of 14 : 1 : 1, 14 : 1 : 2, and 14 : 1 : 3. The bias voltage of all films was set to −5 kV, at an RF power of 300 W. The pulse frequency was set to 1 kHz at a pulse width of 5 μs and a pulse delay of 25 μs, respectively. The deposition pressure was set to 2-3 Pa, and the total deposited thickness of the films was approximately 500 nm. The deposition conditions for the DLC, Si-DLC, and Si-N-DLC films are listed in Table 1.

The film structure was analyzed using Raman spectroscopy (JASCO NRS-1000 DT, beam diameter = 4 μm and wavelength = 532 nm). The Raman spectra in the wavelength of 1,000–1,800 cm^{-1} were deconvoluted into Gaussian D and G peaks. The integral area under the G and D peaks was determined by curve fitting. The composition at the top surface of the films deposited on the silicon substrate was measured using energy dispersive X-ray spectroscopy (EDS). The acceleration voltage was set to 15 kV. The hardness and elastic modulus of the films were measured using a nanoindentation hardness tester. A diamond ball indenter (Berkovich-type) was used with an indentation load of 1,000 μN. The corrosion performance of all films was measured using potentiodynamic polarization experiments in an aqueous 0.05 M NaCl solution. A Pt sheet and Ag/Agcl were used as the counter and the reference electrodes, respectively. The potential voltage was varied from −3 V to +3 V at a scanning rate of 10 mV/s.

3. Results

3.1. Raman Spectra. The Raman spectra obtained are shown in Figures 2-3. The results show the Raman spectra of the pure DLC, Si-DLC, and Si-N-DLC films fabricated at various flow rate ratios, deposited on silicon substrates. The films in this experiment show a broad spectrum composed of a D band

Table 2: G peak and I_D/I_G intensity ratio for all films.

Film type	Gaseous mixture	Gas flow rate ratio	G peak (cm^{-1})	I_D/I_G
Pure DLC	C_2H_2	—	1,534	0.61
Si-DLC	C_2H_2 : TMS	2 : 1	1,479	0.35
		1 : 4	1,457	0.17
Si-N-DLC	C_2H_2 : TMS : N_2	14 : 1 : 1	1,513	0.53
		14 : 1 : 2	1,517	0.57
		14 : 1 : 3	1,520	0.58

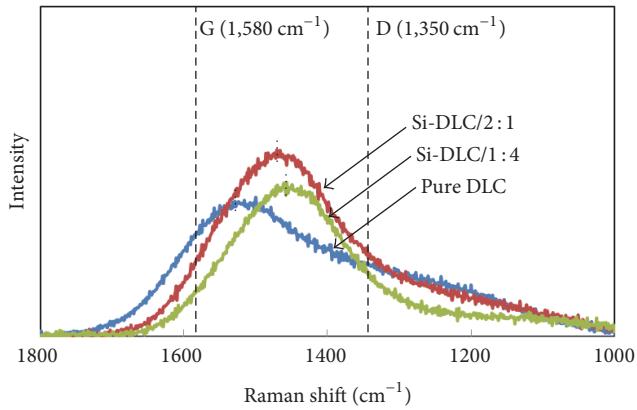

Figure 2: Raman spectra of the DLC and Si-DLC films, at various flow rate ratios.

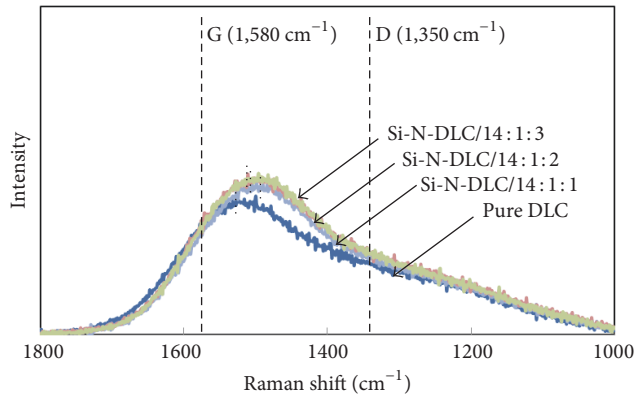

Figure 3: Raman spectra of the DLC and Si-N-DLC films at various flow rate ratios.

(1,350 cm^{-1}) and a G band (1,580 cm^{-1}), which are similar to the peaks observed in conventional DLC films.

From Figures 2-3 and Table 2, the results show that the G peak of the pure DLC film shifted lower, while the I_D/I_G intensity ratio increased with silicon and silicon-nitrogen incorporation. For the Si-DLC film, the G peak shifted from 1,479 cm^{-1} (C : Si/2 : 1) to 1,457 cm^{-1} (C : Si/1 : 4), while the I_D/I_G intensity ratio decreased from 0.35 to 0.17 with silicon incorporation. The G peak shift is believed to be partly due to the changes in the microstructure, that is, formation of more sp^3 clusters with an increase in the silicon contents. Additionally, shifts of the G band position to a lower frequency can be partially attributed to a reduction in the compressive stress when silicon was introduced into the films, because the longer destrained bonds vibrate at a lower frequency [21].

For Si-N-DLC films, the G peak shifts from 1,513 cm^{-1} (C : Si : N/14 : 1 : 1) to 1,520 cm^{-1} (C : Si : N/14 : 1 : 3), while the I_D/I_G intensity ratio increases from 0.53 to 0.58 after silicon-nitrogen incorporation. This is because the incorporation of nitrogen in the DLC film can revert the sp^3 network to a sp^2 network [22]. The G peak shift indicates an increase in the number or size of graphitic domains [23], that is, an increase in sp^2 bonds (sp^3 decreases) and the formation of sp^2 clusters with an increase in the silicon-nitrogen content. These lead to a decrease in the film hardness and elastic modulus.

3.2. Relative Atomic Content. The relative atomic contents measured on the top surface of the films deposited on the silicon substrate are shown in Table 3. The carbon, silicon, oxygen, and nitrogen concentrations were measured using the EDS. Because the hydrogen content could not be measured by EDS, the concentrations were normalized to a total of 100 at.%, neglecting the hydrogen contribution. Moreover, the results show the Si content appeared in the pure DLC film deposited from C_2H_2 precursor gas. This is due to the very thin Si-DLC and Si-N-DLC thickness (approximately 500 nm). It is speculated that the penetration depth of electron during test is higher than 500 nm. Therefore, in terms of qualitative comparison, the estimated Si content on the Si-DLC film is more than almost fourfold compared with that of the Si-N-DLC film.

From Table 3, the results of Si-DLC film show that the Si content increases from 31 at.% to 40 at.% when the gas flow rate ratio changed from 2 : 1 to 1 : 4. The Si-N-DLC film results show that the contents of Si and N gradually increased from 19.3 at.% to 20.2 at.% and 1 at.% to 2 at.%, when the gas flow rate ratio changes from 14 : 1 : 1 to 14 : 1 : 3 (N_2 gas flow increases from 1 sccm to 3 sccm).

3.3. Surface Hardness and Elastic Modulus. The hardness and elastic modulus values of pure DLC, Si-DLC, and Si-N-DLC films deposited on the silicon substrate are shown in Table 3. The results were calculated from a force curve obtained from the nanoindentation hardness test. A diamond ball indenter (Berkovich-type) was used with an indentation load of 1,000 μN.

Table 3: Relative atomic content and mechanical properties of all films.

Film type	Gaseous mixture	Gas flow rate ratio	Relative atomic content (at.%)				Estimated content (at.%)	Mechanical properties	
			C	Si	O	N	Si	Hardness (GPa)	Elastic modulus (GPa)
Pure DLC	C_2H_2	—	84.0	16.0	—	—	—	15.9	142.3
Si-DLC	C_2H_2 : TMS	2 : 1	67.0	31.0	2.0	—	15	13.9	130.8
		1 : 4	57.5	40.0	2.5	—	24	14.4	133.5
Si-N-DLC	C_2H_2 : TMS : N_2	14 : 1 : 1	79.3	19.3	0.40	1.0	3.3	13.7	129.3
		14 : 1 : 2	78.0	19.6	0.90	1.5	3.6	13.3	127.5
		14 : 1 : 3	76.9	20.2	0.90	2.0	4.2	13.0	124.4

Table 4: Electrochemical parameters of all films.

Film type	Gas flow rate ratio	Corrosion potential (E_{corr} (V))	Corrosion current density (i_{corr} (A/cm^2))
Pure DLC	—	−0.19	$-3.05E-11$
Si-DLC	2 : 1	0.44	$-3.92E-11$
	1 : 4	0.61	$-7.05E-11$
Si-N-DLC	14 : 1 : 1	0.85	$-6.43E-11$
	14 : 1 : 2	0.74	$-5.13E-11$
	14 : 1 : 3	0.74	$-5.73E-11$

From Table 3, it is clear that the hardness and elastic modulus of the Si-DLC film gradually increased from 13.9 GPa to 14.4 GPa and 130.8 GPa to 133.5 GPa with silicon incorporation; that is, the Si content gradually increased from 31 at.% to 40 at.%. The increases in the film hardness and elastic modulus are believed to be partly due to the changes in the microstructure, as concluded from the Raman analysis, that is, formation of more sp^3 clusters with an increase in the silicon contents.

For the Si-N-DLC film, the hardness and the elastic modulus gradually decreased from 13.7 GPa to 13.0 GPa and 129.3 GPa to 124.4 GPa with silicon-nitrogen incorporation; that is, the Si and N content gradually increased from 19.3 at.% to 20.2 at.% and 1 at.% to 2 at.%, respectively.

However, a pure DLC film shows the greatest hardness and elastic modulus, although the G peak of the pure DLC film was greater than the Si-DLC and the Si-N-DLC. The high hydrogen content in a pure DLC film prepared from the C_2H_2 precursor gas was speculated to have polymer-like chains, while the greater C content exhibited greater hardness values.

3.4. Corrosion Resistance Property. The potentiodynamic polarization curves of all films are shown in Figure 4. The results obtained from the polarization curves are given in Table 4. In general, the samples in the corrosion behavior with the lower current density and greater potential indicate a better corrosion resistance [24]. An improvement in the corrosion resistance of a film is demonstrated by a shift in the polarization curve towards the region of lower current density and greater potential [24]. Moreover, the difference in the corrosion behavior of the film was attributed to the difference in the microstructure of the films [6]. Generally,

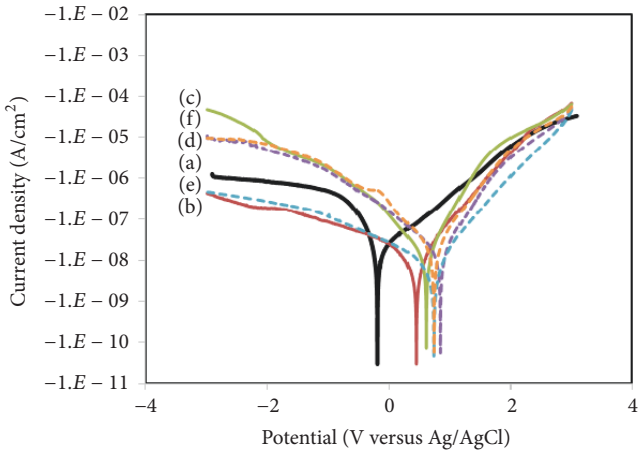

Figure 4: Potentiodynamic polarization of (a) pure DLC, (b) Si-DLC 2 : 1, (c) Si-DLC 1 : 4, (d) Si-N-DLC 14 : 1 : 1, (e) Si-N-DLC 14 : 1 : 2, and (f) Si-N-DLC 14 : 1 : 3.

an increase in the sp^3 bonds in the DLC films reduces the electrochemical corrosion and increases the electrochemical protection efficiency [24, 25].

From Table 4, the results show that the corrosion potential (E_{corr}) of the pure DLC film shifted to a more positive value, while the current density (i_{corr}) decreased with silicon (Si-DLC) and silicon-nitrogen (Si-N-DLC) incorporation. The greater corrosion potential (E_{corr}) and lower current density (i_{corr}) of the Si-DLC and Si-N-DLC films compared with the pure DLC film reveal that the introduction of silicon and silicon-nitrogen into the pure DLC film increases the corrosion resistance because of the increased sp^3 sites in the

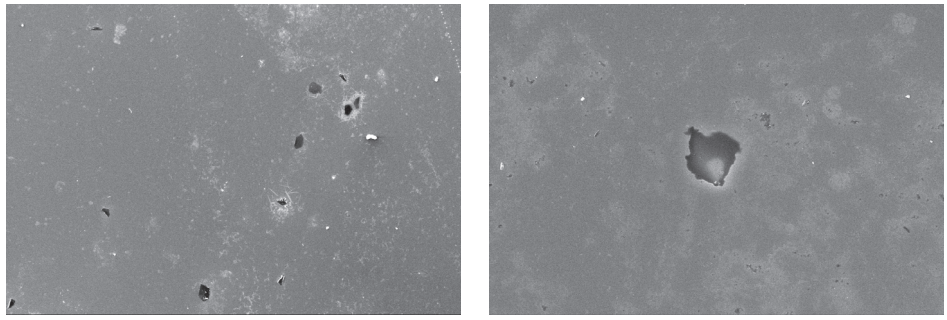

(a) (b)

Figure 5: Pitting corrosion observed with SEM on the DLC film surface after the potentiodynamic tests: (a) 100x; (b) 1,000x.

film [26] and the formation of a passive silicon oxide film [11]. However, although the formation of sp^3 sites caused high internal stress and led to a decrease in the corrosion properties, the incorporation of Si into DLC films stabilized the sp^3 bonding and reduced the stress [10].

For the Si-DLC film, the corrosion potential increased from 0.44 V to 0.61 V, and the current density (i_{corr}) decreased from -3.92×10^{-11} A/cm^2 to -7.05×10^{-11} A/cm^2 with silicon incorporation. For the Si-N-DLC film, corrosion potential decreased from 0.85 V to 0.74 V, and the current density increased from -6.43×10^{-11} A/cm^2 to -5.73×10^{-11} A/cm^2 with silicon-nitrogen incorporation. Therefore, the greatest corrosion potential value of 0.85 V was observed in the Si-N-DLC film with silicon-nitrogen contents of 19.3 at.% Si and 1 at.% N.

Figure 5 shows the surface morphologies of the pure DLC film after the potentiodynamic polarization tests. It is clear that the pits observed on the pure DLC film surface indicate that the pure DLC film is more susceptible to pitting corrosion.

4. Conclusions

Elemental doped diamond-like carbon films (silicon, silicon-nitrogen) were prepared on Si (100) wafers using the PBII technique. The films were investigated in terms of their structures, mechanical properties, and corrosion resistance. It was observed that, by increasing the silicon content in the Si-DLC film, the hardness and corrosion resistance of the film increased. Moreover, by increasing silicon-nitrogen content in the Si-N-DLC film, the hardness and corrosion resistance of the film decreased. The increase and decrease in the film hardness were due to the increases and decrease in sp^3 clusters. The hardness of Si-DLC film can increase to a value of up to 14.4 GPa with a silicon content of 40 at.%, while the hardness of the Si-N-DLC film can increase to value of up to 13.7 GPa with a silicon and nitrogen content of 19.3 at.% and 1 at.%. The corrosion resistance of the pure DLC film increased with the incorporation of silicon (Si-DLC) and silicon-nitrogen (Si-N-DLC). The Si-N-DLC film with silicon and nitrogen contents of 19.3 at.% and 1 at.% showed a corrosion potential value of 0.85 V, which is a considerable improvement.

Conflicts of Interest

The authors declare that they have no conflicts of interest.

Acknowledgments

The authors gratefully acknowledge the financial support provided by King Mongkut's University of Technology Thonburi.

References

[1] S. C. H. Kwok, J. Wang, and P. K. Chu, "Surface energy, wettability, and blood compatibility phosphorus doped diamond-like carbon films," *Diamond and Related Materials*, vol. 14, no. 1, pp. 78–85, 2005.

[2] R. Cruz, J. Rao, T. Rose, K. Lawson, and J. R. Nicholls, "DLC-ceramic multilayers for automotive applications," *Diamond and Related Materials*, vol. 15, no. 11-12, pp. 2055–2060, 2006.

[3] A. Shirakura, M. Nakaya, Y. Koga, H. Kodama, T. Hasebe, and T. Suzuki, "Diamond-like carbon films for PET bottles and medical applications," *Thin Solid Films*, vol. 494, no. 1-2, pp. 84–91, 2006.

[4] Z. Wang, C. Wang, Q. Wang, and J. Zhang, "Electrochemical corrosion behaviors of a-C:H and a-C:N_X:H films," *Applied Surface Science*, vol. 254, no. 10, pp. 3021–3025, 2008.

[5] R. Sharma, P. K. Barhai, and N. Kumari, "Corrosion resistant behaviour of DLC films," *Thin Solid Films*, vol. 516, no. 16, pp. 5397–5403, 2008.

[6] E. Liu and H. W. Kwek, "Electrochemical performance of diamond-like carbon thin films," *Thin Solid Films*, vol. 516, no. 16, pp. 5201–5205, 2008.

[7] N. Huang, P. Yang, Y. X. Leng et al., "Surface modification of biomaterials by plasma immersion ion implantation," *Surface and Coatings Technology*, vol. 186, no. 1-2, pp. 218–226, 2004.

[8] G. Q. Yu, B. K. Tay, and Z. Sun, "Fluorinated amorphous diamond-like carbon films deposited by plasma-enhanced chemical vapor deposition," *Surface and Coatings Technology*, vol. 191, no. 2-3, pp. 236–241, 2005.

[9] L. Xia, M. Sun, and J. Liao, "The effect of negative bias pulse on the bonding configurations and properties of DLC films prepared by PBII with acetylene," *Diamond and Related Materials*, vol. 14, no. 1, pp. 42–47, 2005.

[10] P. Papakonstantinou, J. F. Zhao, P. Lemoine, E. T. McAdams, and J. A. McLaughlin, "The effects of Si incorporation on the

electrochemical and nanomechanical properties of DLC thin films," *Diamond and Related Materials*, vol. 11, no. 3-6, pp. 1074–1080, 2002.

[11] M. Azzi, P. Amirault, M. Paquette, J. E. Klemberg-Sapieha, and L. Martinu, "Corrosion performance and mechanical stability of 316L/DLC coating system: Role of interlayers," *Surface and Coatings Technology*, vol. 204, no. 24, pp. 3986–3994, 2010.

[12] J. Choi, S. Nakao, J. Kim, M. Ikeyama, and T. Kato, "Corrosion protection of DLC coatings on magnesium alloy," *Diamond and Related Materials*, vol. 16, no. 4–7, pp. 1361–1364, 2007.

[13] J. Choi, J. Kim, S. Nakao, M. Ikeyama, and T. Kato, "Friction properties of protective DLC films on magnesium alloy in aqueous NaCl solution," *Nuclear Instruments and Methods in Physics Research, Section B: Beam Interactions with Materials and Atoms*, vol. 257, no. 1-2, pp. 718–721, 2007.

[14] J. Choi, S. Nakao, M. Ikeyama, and T. Kato, "Effect of deposition pressure on the properties of DLC coatings deposited by bipolar-type PBII&D," *Surface and Interface Analysis*, vol. 40, no. 3-4, pp. 806–809, 2008.

[15] A. Zeng, E. Liu, S. N. Tan, S. Zhang, and J. Gao, "Stripping voltammetric analysis of heavy metals at nitrogen doped diamond-like carbon film electrodes," *Electroanalysis*, vol. 14, no. 18, pp. 1294–1298, 2002.

[16] R. Hatada, S. Flege, A. Bobrich, W. Ensinger, and K. Baba, "Surface modification and corrosion properties of implanted and DLC coated stainless steel by plasma based ion implantation and deposition," *Surface and Coatings Technology*, vol. 256, pp. 23–29, 2014.

[17] I. Masami, N. Setsuo, S. Tsutomu, and C. Junho, "Improvement of corrosion protection property of Mg-alloy by DLC and Si-DLC coatings with PBII technique and multi-target DC-RF magnetron sputtering," *Nuclear Instruments and Methods in Physics Research, Section B: Beam Interactions with Materials and Atoms*, vol. 267, no. 8-9, pp. 1675–1679, 2009.

[18] N. Moolsradoo and S. Watanabe, "Deposition and tribological properties of sulfur-doped DLC films deposited by PBII method," *Advances in Materials Science and Engineering*, Article ID 958581, 7 pages, 2010.

[19] N. Moolsradoo and S. Watanabe, "Modification of tribological performance of DLC films by means of some elements addition," *Diamond and Related Materials*, vol. 19, no. 5-6, pp. 525–529, 2010.

[20] N. Moolsradoo, S. Abe, and S. Watanabe, "Thermal stability and tribological performance of DLC-Si–O films," *Advances in Materials Science and Engineering*, Article ID 483437, 7 pages, 2011.

[21] J. Meneve, E. Dekempeneer, W. Wegener, and J. Smeets, "Low friction and wear resistant a-C:H/a-$Si_{1-x}C_x$:H multilayer coatings," *Surface and Coatings Technology*, vol. 86-87, no. 2, pp. 617–621, 1996.

[22] S. C. Ray, W. F. Pong, and P. Papakonstantinou, "Iron, nitrogen and silicon doped diamond like carbon (DLC) thin films: a comparative study," *Thin Solid Films*, vol. 610, pp. 42–47, 2016.

[23] F. L. Freire Jr., G. Mariotto, R. S. Brusa, A. Zecca, and C. A. Achete, "Structural characterization of amorphous hydrogenated carbon and carbon nitride films deposited by plasma-enhanced CVD," *Diamond and Related Materials*, vol. 4, no. 4, pp. 499–502, 1995.

[24] J. H. Sui, Z. G. Zhang, and W. Cai, "Surface characteristics and electrochemical corrosion behavior of fluorinated diamond-like carbon (F-DLC) films on the NiTi alloys," *Nuclear Instruments and Methods in Physics Research Section B: Beam Interactions with Materials and Atoms*, vol. 267, no. 15, pp. 2475–2479, 2009.

[25] A. C. Ferrari and J. Robertson, "Interpretation of Raman spectra of disordered and amorphous carbon," *Physical Review B*, vol. 61, no. 20, pp. 14095–14107, 2000.

[26] N. W. Khun, E. Liu, and X. T. Zeng, "Corrosion behavior of nitrogen doped diamond-like carbon thin films in NaCl solutions," *Corrosion Science*, vol. 51, no. 9, pp. 2158–2164, 2009.